Nanoscale

Accepted Manuscript

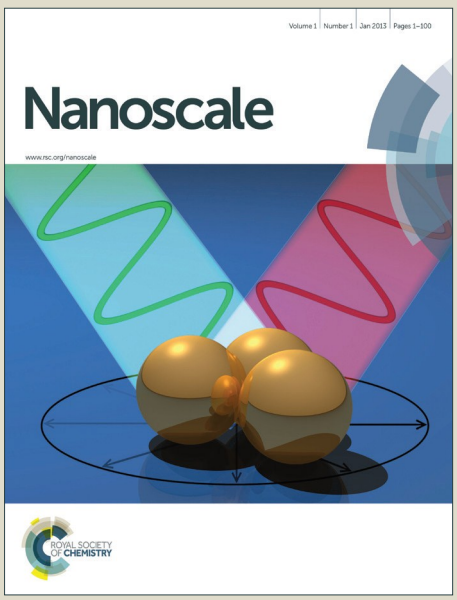

This is an *Accepted Manuscript*, which has been through the Royal Society of Chemistry peer review process and has been accepted for publication.

Accepted Manuscripts are published online shortly after acceptance, before technical editing, formatting and proof reading. Using this free service, authors can make their results available to the community, in citable form, before we publish the edited article. We will replace this *Accepted Manuscript* with the edited and formatted *Advance Article* as soon as it is available.

You can find more information about *Accepted Manuscripts* in the Information for Authors.

Please note that technical editing may introduce minor changes to the text and/or graphics, which may alter content. The journal's standard Terms & Conditions and the Ethical guidelines still apply. In no event shall the Royal Society of Chemistry be held responsible for any errors or omissions in this *Accepted Manuscript* or any consequences arising from the use of any information it contains.

ROYAL SOCIETY OF CHEMISTRY

www.rsc.org/nanoscale

Please do not adjust margins

Nanoscale

Paper

Heteroaggregation Assisted Wet Synthesis of Core-Shell Silver-Silica-Cadmium Selenide Nanowires

I. A. Pita,[a] S. Singh[b], C. Silien[a], K. M. Ryan[b] and N. Liu*[a]

Received 00th January 20xx,
Accepted 00th January 20xx

DOI: 10.1039/x0xx00000x

www.rsc.org/

A method has been developed for the wet solution synthesis of core shell heterogeneous nanowires. An ultrathin silica layer was first grown around plain silver nanowires to act as a suitable insulator. An outer nanoparticle layer was then attached through heteroaggregation by dispersing the un-functionalized nanowires in toluene solutions containing nanoparticles of CdSe or Au. Total coverage of nanoparticles on nanowires was found to increase with the nanoparticle size, which is attributed to the increase in the van der Waals interaction between the nanoparticles and the nanowire with the increasing size of nanoparticles. Using this method, we achieved over 79.5% coverage of CdSe nanoparticles (24 nm × 11 nm) on the nanowire surface. Although following the same trend, Au nanoparticles however show an overall lower coverage than CdSe, with only 24.2% coverage at their largest particle size of 19 nm in diameter. This result is attributed to the increase in surface repulsion during attachment due to the increasing length of capping ligands. Investigation of the core-shell nanowire's optical properties yielded CdSe Raman peak enhancement by a factor of 2-3 due to the excitation of surface plasmon propagation. Our method can be applied to the attachment of a wide range of nanoparticles to nanowire materials in non-polar solution and the core-shell nanowires show great potential for incorporation into various microscopic and drug delivery applications.

Introduction

Metallic nanowires, due to their various applications in optoelectronic devices, have been studied extensively in recent years. In particular, silver nanowires have demonstrated applications as probes for general optical sensing[1] such as fluorescence microscopy and as the building blocks for nanocircuits[2-4]. Silver nanowires have also found applications as drug delivery systems. As an example, research has shown that suitably functionalized nanowires could be used to penetrate and treat cells in lung cancer patients[5].

Heterogeneous (metal/semiconductor (insulator)) materials show potential benefits over plain metal structures due to interactions between the different material layers. One of these interactions is surface plasmon propagation; where light of a suitable frequency causes coherent electron oscillations to propagate along the metal/semiconductor (insulator) interface. This propagation produces an electromagnetic wave which decays exponentially into the material from the surface[6]. Due to the interplay between different materials present in heterogeneous structures, some optical or electrical properties can be altered or enhanced. As an example of this, heterogeneous nanobelts of metal-insulator-semiconductor layered structures have proven capable of producing hybrid plasmonic modes for signal amplification[7] and lasers[8], while gold-PbS nanocubes can produce response times suitable for the formation of saturable absorbers[9]. The incorporation of semiconductor or other functioning material at the vicinity of metallic nanowires can greatly enhance their applications in optical sensing and drug delivery.

Heteroaggregation, the attachment of dis-similar particles in solution[10,11], has previously been used to coat spherical particles with dis-similar outer nanoparticle layers such as polymer microbeads coated with gold, silver, or semiconductor material[12,13]. Studies have indicated that the particles adsorbed on the surface show a preference for lateral attachment over clustering on the surface, and that the attachment process can begin at lower energies compared to bulk aggregation[14]. In some cases the heteroaggregation allows complete monolayer particle shells to be formed outside a larger diameter particle completely. While heteroaggregation has been studied extensively on spherical particles in aqueous solution, the effect of particle interactions in nonpolar solvent and between nanoparticles and a cylindrical nanowire structure remains relatively unknown.

In this paper a novel synthesis route is developed for the formation of a metal-insulator-semiconductor and metal-insulator-metal core-shell nanowire, utilizing heteroaggregation as the final step to attach an outmost semiconductor cadmium selenide (CdSe) or Au nanoparticle layer in toluene. Silver nanowires were synthesized to act as the metal core, and a thin insulating layer of silica was then grown using a modification to the well-known Stöber method[15-18], originally used for the synthesis of uniform silica spheres. The heteroaggregation step was carried out by dispersing the nanowires in solutions of toluene containing nanoparticles of either CdSe or Au to investigate metal-insulator-semiconductor, and metal-insulator-metal nanowire structures. In both cases the silica coated silver nanowires were not functionalized. Larger CdSe nanoparticles were

[a] Department of Physics and Energy, Materials and Surface Science Institute, University of Limerick Ireland.
[b] Department of Chemical and Environmental Science, Materials and Surface Science Institute, University of Limerick, Ireland.

Electronic Supplementary Information (ESI) available: Nanoparticle Synthesis, van der Waals calculations, Optical data from the core-shell nanowires along with individual nanoparticle contribution determination, and comparison of Raman band data with COMSOL simulations. See DOI: 10.1039/x0xx00000x

Nanoscale Accepted Manuscript

Please do not adjust margins

capped with tetradecylphosphonic acid, while the Au, and smaller CdSe, nanoparticles were capped with oleylamine and/or oleic acid.

Results obtained indicated that for the CdSe nanoparticles the coverage was critically dependent on the size of the particles, with larger nanoparticles capable of covering the majority of the wire's surface (80 percent) and smaller nanoparticles showing continuous reductions in coverage, while Au nanoparticles were seen to exhibit a similar trend but in general with lower coverage to that seen for the CdSe nanoparticles. Because the nanoparticles are weakly charged[19-21], we attribute the size dependent coverage change to the increases in the van der Waals interaction between the nanowire and nanoparticle following the increase of particle size, with steric repulsion, originated from Pauli Exclusion Principle, being the other major contributing factor. Together, these two interactions form an energy well to trap the nanoparticles at the nanowire surface. Particle attachment is modelled after a particle attachment-detachment rate equation, with a saturation point that was reached when particle movement reaches an equilibrium point. When illuminated with a 532 nm laser Raman spectra of the wires were also found to match those of plain CdSe. With a specific excitation configuration, this led to increases in the Raman signal per nanoparticle, highlighting the effects of excited surface plasmons. The completed structure shows potential for use as a probe in certain microscopic techniques and as a suitable system for metallic nanowire based drug delivery studies.

Experimental

Silver nanowires 2-10 µm long were synthesized using soft solution phase synthesis[22] to form the core of the heterogeneous nanowire. The synthesized wires were stored in ethelyne glycol, making them stable for more than six months.

The growth of the ultrathin silica layer was achieved through a new modification to the Stöber method. 0.5-2 mL of the silver nanowire solution (20- 75 mg of silver nanowires approx.) was first washed four times with isopropanol under centrifuge at 3100 rpm. The washed wires were then functionalized by dispersing them into a 4: 1 de-ionized water: isopropanol mixture containing 60 mg 4-mercaptobenzoic acid previously dissolved in 2 mL isopropanol. The solution was left under 500 rpm magnetic stirring for 1 hour. Following this step, the wires were again washed with isopropanol twice under centrifuge at 3500 rpm and re-dispersed into a new 4 : 1 de-ionized water : isopropanol mixture in a three neck flask. The solution was stirred at 500 rpm in a nitrogen atmosphere at room temperature. In order to grow the silica layer, 0.15 mL of ammonium hydroxide was then injected into the solution followed by 0.024 g of tetraetheylorthosilicate. The reaction was left for 1 hour. The wires were then washed a further four times under centrifuge, to halt the silica growth, and were stored in 10 mL of isopropanol.

In order to attach the outer layer of nanoparticles via heteroaggregation, cadmium selenide nanoparticles of different sizes were synthesized: 6 nm in diameter from a new synthesis procedure (see supplementary information), and 15 nm × 9 nm, along with 24 nm × 11 nm sizes (in all cases the dimensions are length by diameter) by changing the amounts of reactants as stated in the reference[23,24]. Au nanoparticles were also synthesized (10 nm diameter, and 19 nm diameter in size[25]) to test the feasibility of metal-insulator-metal wires. The termination ligand for the larger CdSe nanoparticles was tetradecylphosphonic acid, while the smallest CdSe nanoparticle and the Au nanoparticles had oleic acid. Prior to use the CdSe nanoparticles were washed in toluene and isopropanol to remove most ligands. The Au nanoparticles were not washed due to the risk of homoaggregation caused by isopropanol. Each type of nanoparticle was then dispersed into 10 mL toluene solutions; for CdSe a weight per volume of 4.8 mg/ mL was used for all different sized particles, while the Au nanoparticles had a higher measure of 30 mg/ mL to account for the mass of the gel matrix. The particles needed to remain as monodisperse as possible when dispersed into the toluene, as homoaggregation was found to reduce the level of coverage achievable on the wire surface. 3 mL of the solution containing silica coated nanowires are then added to each particle solution and sonicated for 5-10 minutes three times a day, at eight hour intervals, for 20 days. At different points during this period the wires were washed out through centrifuge with isopropanol to inspect coverage of the wires.

Results and discussion

An example of a completed core shell silver-silica-CdSe nanowire through each stage of its fabrication is shown in Fig. 1. Analysis of the nanowires under TEM after the silica growth step revealed that an ultrathin silica layer 5-10 nm thick had been successfully grown around more than 95 % of the nanowires. The inspected layers were quite smooth with only occasional flaking seen, and the thickness was between 5 to 10 nm, sufficient to be used as an insulating layer.[5] If a thicker layer was desired; however, the amount of tetraethylorthosilicate can be increased in the growth step, or by decreasing wire concentration. The total coverage of the CdSe and Au nanoparticles were inspected under SEM. It was found that the CdSe nanoparticles yielded the best results with sharp increases in average coverage seen for increasing particle size.

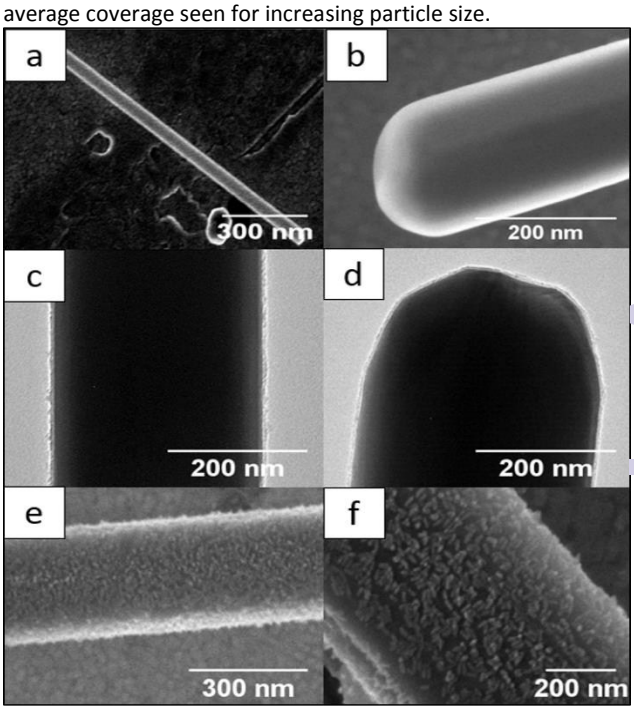

Fig. 1: (a) + (b) Plain silver nanowires, (c) + (d) silver nanowires coated with silica, (e) + (f) silica coated silver nanowire coated with 24 nm x 11 nm CdSe nanoparticles.

This increase is seen from a 22.0 ± 9.7 % average for the 6 nm long nanoparticles to 40.8 ± 15.9 % for the 15 nm, and an overall maximum average of 79.5 ± 11.3 % for the 24 nm ones, with a good number of nanowires with over 90 % coverage. In addition

Nanoscale Accepted Manuscript

This journal is © The Royal Society of Chemistry 2015

increase in the particle size shows a continual reduction in the number of uncoated wires. Fig. 2 shows the coverage obtainable for thirty nanowires after 3 days in solution from each case, which highlights the continuous increases in coverage with size. An increase was also seen for the Au nanoparticles, but to a smaller extent with an approximate increase of only 2 % for the 19 nm nanoparticles, as seen in fig. 3. At saturation the nanowires only achieve coverage of 24.2 ± 6.3 % and 22.1 ± 8.1 % for the 19 nm and 10 nm nanoparticles respectively.

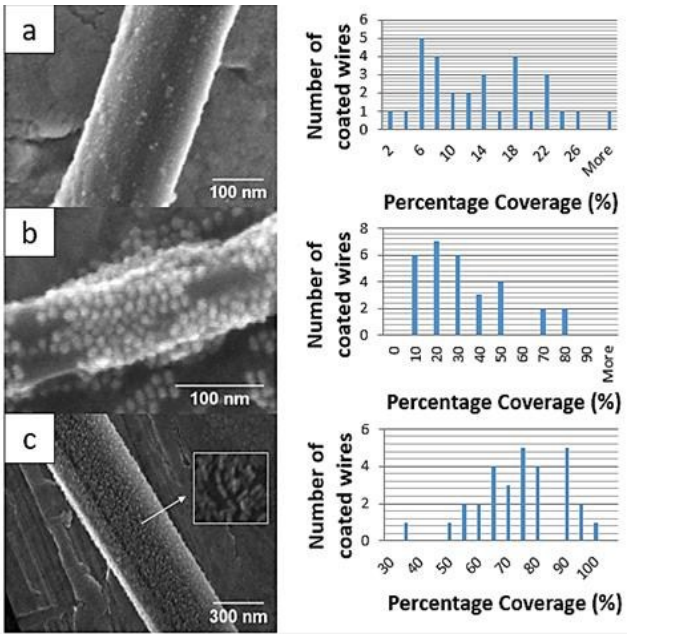

Fig. 2: An image of an averagely coated nanowire, and the percentage coverage recorded for 30 nanowires in histogram form, after a period of 3 days for (a) 6 nm x 6 nm, (b) 15 nm x 9 nm, and (c) 24 nm x 11 nm CdSe nanoparticles. Images obtained using SEM.

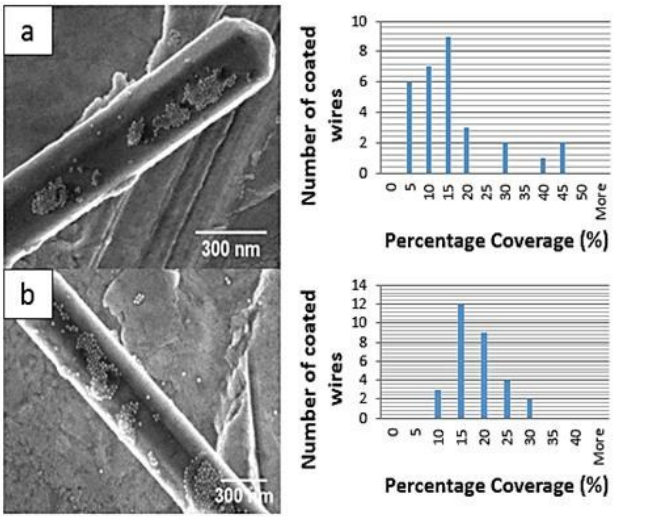

Fig. 3: An image of an averagely coated nanowire, and the percentage coverage recorded for 30 nanowires in histogram form, after a period of 3 days for (a) 10 nm diameter, and (b) 19 nm diameter Au nanoparticles. Images obtained using SEM.

van der Waals and Steric Repulsion Contributions

The increase in coverage of nanoparticles on the wires is attributed to the increase in the magnitude of total interaction energy of the system. The double layer forces are not considered relevant here as the charge associated with nonpolar solvent toluene is much lower than that of other aqueous liquids such as water. As a result, its effects are thought to be minimal. Instead, van der Waals force is considered as the major attractive force, which is dependent on the dimensions of the particle[26]. In our study, all particles are terminated with long chain ligands. As the distance between the nanoparticle and silver nanowire decreases, steric repulsion due to the compression to the ligand shell of the nanoparticle becomes important. The combined effect of these two forces lead to the formation of an energy well that stabilizes the nanoparticles at a close vicinity of the nanowire. Both forces are much stronger at short range, with the strength decaying as the nanoparticles move further away.

Here an estimation of the van der Waals interaction energy is made for both the CdSe and Au cases. Three components are considered to determine the attractive energy experienced by the nanoparticle (see figure 4): (1) the nanoparticle's interaction with the silver nanowire over the silica interface, (2) the nanoparticle's interaction with the ultrathin silica layer, and (3) the opposing attraction that the nanoparticle experiences from the toluene. The silica coated silver nanowires are taken as cylinders with average length of 5 µm and diameter 235 nm. Calculation of the Hamaker coefficient (A_H) can be obtained using the combining relations for Hamaker coefficients[26,27]:

$$A_{131} \approx (\sqrt{A_{11}} - \sqrt{A_{33}})^2 \quad (1)$$

$$A_{132} \approx (\sqrt{A_{11}} - \sqrt{A_{33}})(\sqrt{A_{22}} - \sqrt{A_{33}}) \quad (2)$$

Where A_{132} is the Hamaker coefficient for phase 1 and phase 2 interacting in a medium 3, as shown in figure 4, allows estimation of the constant for CdSe-silica-silver and Au-silica-silver. A_{11}, A_{22} and A_{33} indicate cases where a phase interacts with itself across a vacuum. In effect, A_{11} would match the case A_{131} if the medium it was interacting across was vacuum. For these calculations the values are available from literature sources. In the calculations to compute parts (1) and (2) the effects of the toluene were ignored as the silica layer is ultrathin and acts as more of a medium to the particle attachment. In addition, the toluene system was calculated separately in part (3). Hamaker coefficient values of 34.20×10^{-20} J for silver-vacuum-silver, 6.55×10^{-20} J for silica-vacuum-silica[28], 45.00×10^{-20} J for Au-vacuum-Au[29,30], and a CdSe-vacuum-CdSe value of 15.60×10^{-20} J[31] were used when determining the Hamaker coefficients for the system. This yielded a Hamaker coefficient of 4.57×10^{-20} J for CdSe-silica-silver. The Hamaker coefficient for Au-silica-silver was calculated as 13.64×10^{-20} J.

In order to calculate the Hamaker's coefficients for the CdSe and Au nanoparticles' interaction with toluene (part (3)) or with silica (part (2)) one further combination relation was used[26]:

$$A_{12} \approx (\sqrt{A_{11}A_{22}}) \quad (3)$$

A Hamaker coefficient value of 5.4×10^{-20} J, obtained from literature[32], was used for toluene-vacuum-toluene in these calculations. Using this equation values of 9.18×10^{-20} J and 10.10×10^{-20} J were obtained for CdSe-toluene and CdSe-silica respectively. Similarly values of 15.58×10^{-20} J and 17.17×10^{-20} J were calculated for Au-toluene and Au-silica.

Nanoscale Accepted Manuscript

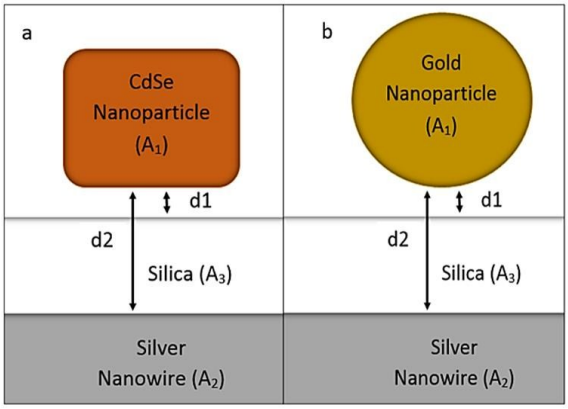

Fig. 4: Representation of the two cases used when calculating the van der Waals interaction energy for both (a) a CdSe nanoparticle, and (b) an Au nanoparticle. The distance of the nanoparticle to the silica is represented as d1. The distance of the nanoparticle from the silver is represented as d2, and takes into account the thickness of the silica layer. A_1, A_2, and A_3 represent the Hamaker coefficient of the material. For the Hamaker coefficient A_{132}, this would mean the interaction of the nanoparticle with the silver nanowire through the silica layer.

Approximating the three sizes of CdSe nanoparticles as cylinders allows for the calculation of the van der Waals interaction energy per unit length of the nanoparticle when the long axis of the nanorods are parallel with the long axis of the nanowire using the Derjaguin approximation[26,33]:

$$Energy_{VdW} = \frac{-A_{132}}{12\sqrt{2}D^{\frac{3}{2}}}\left(\frac{R_1R_2}{R_1+R_2}\right)^{\frac{1}{2}} \quad 4$$

While both cylinders perpendicular follow the equation:

$$Energy_{VdW} = \frac{-A_{132}\sqrt{R_1R_2}}{6D} \quad 5$$

Where D is the separation between the cylinders (d1 or d2 depending on the system being calculated, and R_1 and R_2 are the radii of the nanoparticle and the nanowire respectively. The Derjaguin approximation was considered valid in these cases, as the nanowire's radius is much greater than that of the distance between the particle and the nanowire surface. Furthermore, the silica coated silver nanowire was also taken as flat surface in separate calculations to determine if the radius was large enough to behave as if completely flat. In the calculations the cylinder configuration would match that of the parallel case above. This was calculated as[26,33]:

$$Energy_{VdW} = \frac{-A_{132}\sqrt{R}}{12\sqrt{2}D^{\frac{3}{2}}} \quad 6$$

Here R indicates the radius of the nanorod. The values obtained from equations 4 and 6 were per unit length, meaning that the actual energy value was determined by multiplying by the length of the nanorods. The dimensions of the nanoparticles in comparison to the distance from the nanowire, (with the distance to the silica being relatively small) was believed to further reduce error.

Two different distances were used when calculating the van der Waals energy of the system (see fig.4); d1 was taken as the distance from the nanoparticle to the silica layer, as well as the distance to the toluene in solution (in (part 3)). The distance from the nanoparticle to the silver was taken as d2, including the thickness of the silica. In these calculations the thickness of the silica was taken as an average of 7.5 x 10^{-9} m.

The values for the nanorod when parallel, perpendicular, and regarding the nanowire as a flat plate were found to be quite similar. van der Waals values for the parallel and flat plate configurations were almost identical, while the perpendicular case was in the same order of magnitude as the other cases. This held regardless of what values of d1 and d2 were chosen to be put into the equations for the three configurations, something which has proven true in previous investigations between spherical particles and cylinders for EDL energies[34] due to the large nanowire radius. Due to both configurations being reasonably close to the flat plate approximation, it is believed that the majority of the nanoparticles behave as if on a flat surface.

For the Au nanoparticles the system is taken as a sphere and cylinder (nanowire). The van der Waals interaction of such a system can be expressed as[34,35]:

$$Energy_{VdW} = \frac{-16A_{132}R_1^3}{3\pi}\int_0^{\pi} d\varphi \int_0^{R_2} \rho d\rho \int_0^{L} [(D+R_1+R_2 + \rho cos\varphi)^2 + (\rho sin\varphi)^2 + z^2 - R_1^2]^{-3} dz \quad 7$$

where L is the length of the cylinder, and R_1 and R_2 are the radii of the nanoparticle and the nanowire respectively. Due to the ratio of the cylinder radius to that of the nanoparticles being greater than 10 it is possible, however, to estimate the energy and force through a more straightforward sphere flat surface calculation. Due to the shape of the Au nanoparticles, and the complete energy of the system being obtained from the radius of the nanoparticles alone, the surface element integration (SEI) approximation was used to reduce error in the estimation of the van der Waals interaction energy[36]:

$$Energy_{VdW} = \frac{-A_{132}}{6}\left[\frac{R_1}{D} + \frac{R_1}{D+2R_1} + \ln\left[\frac{D}{D+2R_1}\right]\right] \quad 8$$

For a nanoparticle fully immersed in toluene, we assume that its interaction energy with toluene is zero. The interaction with the 7.5 nm silica (which is the average silica layer thickness) was estimated by varying the distance between a nanoparticle and a silica block. In order to calculate the interaction energy between the nanoparticles attached to the nanowire and the toluene (part 3), the interaction is estimated as if the nanoparticle is interacting with a large block of toluene with a distance d1 from the particle. The total van der Waals energy was than obtained by summing the individual energies for material-silica-silver (1) and material-silica (2), and subtracting material-toluene (3).

As discussed previously, the main contribution to the repulsion of the nanoparticles is considered the steric repulsion. The physical origin of the steric repulsion is from Pauli Exclusion Principle. Once the atoms within or between the molecules are brought too close together, there is an associated energy cost due to the overlapping of electron clouds. Steric repulsion occurs when the interfacial layers of two colloids overlap, causing a repulsive force[32]. In our case, steric repulsion needs to be considered when the ligand layer is compressed too much due to the decrease of nanoparticle-nanowire distance. The energy of steric repulsion can be calculated, to a first approximation, as[37]:

$$E_{steric} = \left(\frac{\delta}{d1}\right)^{12} k_bT \quad 9$$

where δ is the thickness of the interfacial layer, k_b is Boltzmann's constant, d1 is the distance between the nanoparticle and nanowire and T is the temperature. For these calculations a factor of two is ignored, as the nanoparticles are interacting with the nanowires, n

Nanoscale Accepted Manuscript

This journal is © The Royal Society of Chemistry 2015

identical particles, and the silica does not have an interfacial layer. The $(d1)^{-12}$ term closely resembles the repulsive term in Lennard-Jones potential, which again reflects the nature of this force. In order to determine the effects of the steric repulsion, the entire energy of the system was estimated using Boltzmann distribution statistics. The Boltzmann distribution is used to determine the probability P(i) that a particle is in a particular energy state, which can be written as[38]:

$$P(i) = Ae^{\frac{-E_i}{k_b T}} \qquad 10$$

Here E_i is the energy of the state, and A is a constant determined from the partition function. Here we assume that the particle in the toluene solution has zero energy, so that the attached particles on the nanowire are in a lower state. In order for the particles to go into the solution, they need to escape from the potential well. The deeper the well is, the harder it is to escape, and the higher the coverage is. The obtained percentage coverage was used as the probability that the nanoparticle would remain on the surface. This value is then used to determine the energy required for the system to have this percentage of nanoparticles leaving the wire's surface. The difference between the obtained energy, and the van der Waals interaction energy was then taken as the steric repulsion energy. In order to calculate both the optimum distance from the nanowire surface, and interfacial layer thickness, the distance between the nanoparticle and the wire surface d1 was altered, along with the interfacial layer thickness, until the correct total energy value was obtained from the calculated van der Waals and steric energy. When calculating the van der Waals energy the value of d2 was increased by d1 each time to account for the increasing distance from the nanowire. The chain length of the capping molecules was estimated from the molecular formula, and the length of C-H, and phosphate ion bonds. The length of tetradeclyphosphonic acid was calculated as 1.68 nm, while the calculated length of oleic acid was 1.97 nm. The temperature was taken as 293 K for these calculations.

The fitted interfacial layer thickness for the Au nanoparticles was found to be a perfect match to the calculated chain length of oleic acid at 1.97 nm. For the larger 24 nm and 15 nm CdSe the calculated value was at 1.47 nm and the 6 nm CdSe the value was 1.34 nm. These two values are smaller than those of the chain lengths but are reasonable considering all CdSe nanoparticles were washed 2 times before use, and less ligands were attached to the particles, leading to smaller effective interfacial layer thicknesses.

The calculated values for the total energy of the system, along with the optimum distance and the determined van der Waals and steric repulsion values are shown in table 1. The results obtained support the theory that the larger nanoparticles would have a much stronger attractive energy; making them less susceptible to thermal excitation, and increasing the total coverage. As a comparison, we also calculate the Coulomb interaction energy between the nanoparticle and silver nanowire. The charge on individual CdSe nanoparticle is estimated to be 0.2e ~ 0.4e based on our previous study[20]. The Coulomb interaction energy for all particle sizes has been estimated to be in the range of -0.4 to -2 $\times$ 10^{-22} J. (See supplementary information for details) These values are one order of magnitude lower than that the van der Waals interaction. As such, its effects on the nanoparticle-nanowire attachment are minimal.

The largest CdSe nanoparticles have a much larger van der Waals energy at -10.47 x 10^{-21} J, which is much higher in magnitude than the standard thermal excitation at room temperature estimated at around 4.04 x 10^{-21} J, making them much more likely to remain on the nanowire's surface. This was also found to be true for the 15 nm CdSe and 19 nm Au nanoparticles. In comparison the 10 nm Au and 6 nm CdSe nanoparticles have much smaller van der Waals values at -3.47 x 10^{-21} J and -1.16 x 10^{-21} J respectively. These values are lower in magnitude than the thermal excitation (k_bT), making them more likely to be excited from the nanowire surface before steric repulsion is even considered. The optimum fitted distance is also seen to reduce with increasing particle size; the larger nanoparticles can come closer to the surface then the smaller ones.

The effect of the interfacial layer thickness can be seen clearly through comparison with the Au nanoparticles. The Hamaker coefficient for Au-silica-silver is larger than that of CdSe-silica-silver. However, due to the much longer capping agent used in the synthesis the optimum distance for the 19 nm Au nanoparticle is 1.93 nm. This substantially reduces the nanoparticle's van der Waals interaction energy to -6.56 x 10^{-21} J. As a result surface coverage is much lower. Yet, when compared to the 10 nm Au nanoparticles, the other nanoparticle with the same thickness oleic acid ligand, it still comes much closer to the wire's surface. In addition the trend in nanoparticle size is once again apparent, with the optimum distance increasing with the nanoparticle dimensions.

The effect on distance overall for both the obtained van der Waals energy and steric repulsion is shown in fig. 5 for the 24 nm x 11 nm CdSe nanoparticle case. In the figure the potential well for the 24 nm CdSe nanoparticles is clearly visible in the region of 1.5 nm to 2.5 nm. As shown in the figure, increasing the distance causes the steric repulsion to reduce extremely quickly towards zero. The van der Waals values also decrease but at a reduced rate overall.

Table 1: The calculated total interaction energy from the coverage, along with the van der Waals and steric repulsion, calculated from the optimum distance, for the various nanoparticles used. The optimum fitted distance to obtain the observed coverage is included for reference.

Nanoparticle size	Total Energy of the System ($\times$ 10^{-21} J)	Optimum Distance (nm)	van der Waals Interaction Energy ($\times$ 10^{-21} J)	Steric Repulsion ($\times$ 10^{-21} J)
24 nm x 11 nm CdSe	-6.41	1.47	-10.47	4.04
15 nm x 9 nm CdSe	-2.12	1.48	-5.82	3.73
6 nm x 6 nm CdSe	-1.00	1.80	-1.17	0.17

Nanoscale Accepted Manuscript

19 nm Au	-1.16	1.93	-6.56	5.34
10 nm Au	-1.06	2.06	-3.47	2.36

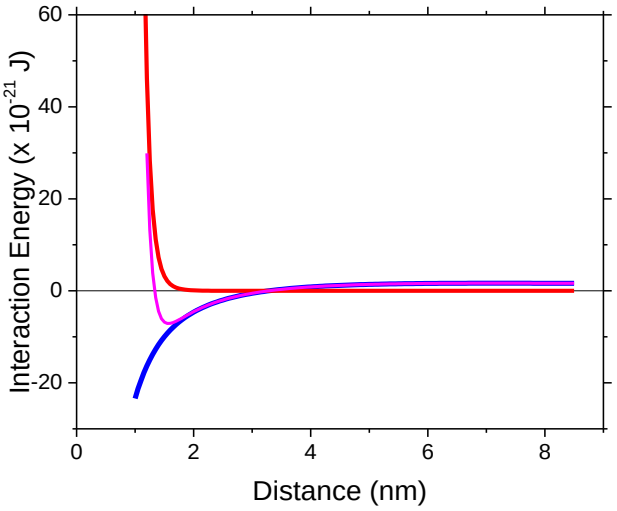

Fig. 5: The (blue) van der Waals interaction energy and (red) steric repulsion for different distances in the 24 nm x 11 nm CdSe nanoparticle case. The purple line shows the total energy obtained when the van der Waals and steric repulsion values are added together. The black line represents absolute zero.

Additionally, the strength of the repulsive energy at short range helps highlight the issue with the longer chain interfacial layers of the Au nanoparticles. Decreasing the distance past the interfacial layer thickness of the nanoparticles causes steric repulsion such that particle attachment would be much more difficult. Due to this fact, the nanoparticles could not get as close to the surface as the larger CdSe nanoparticles.

These results indicate that both the nanoparticle size, and interfacial layer thickness are the major factors effecting coverage. While the larger CdSe nanoparticles experience a similar steric repulsion, the stronger van der Waals interaction energy of the 24 nm x 11 nm ones give the nanoparticles a much stronger preference to remain on the surface. In addition, the shorter capping molecules mean that, at the same distance, the system is overall more likely to shift towards surface attachment than the longer molecules.

Deposition Rate Coefficient

The entropy of mixing (or configuration entropy) is the main driving factor for the nanoparticle attachment to start when the bare SiO_2 coated Ag nanowires are transferred in to the nanoparticle solution. Monitoring of the average particle attachment every few days allowed for the change in particle attachment with time to be studied. Analysis of these results indicated an initial increase in the average coverage of nanowires before a saturation point was reached which usually occurred within the first 5 days in solution. The saturation is thought to be due to the attachment-detachment rate of particles reaching an equilibrium point, where the number of additional nanoparticles attaching to the surface becomes equal to those detaching. While previous studies of heteroaggregation have included the effects of homoaggregation on particle attachment such as the Von Smoluchowski-Stokes equation[39], it is ignored here as the particles only attached to the surface as monolayers, and the majority of nanoparticles did remain monodisperse in solution. The general curves obtained can then be readily fit to a standard particle attachment-detachment rate equation[40]:

$$\frac{\partial B}{\partial \mathrm{t}} = k_a C(B_0 - \mathrm{B}) - k_d B \qquad 11$$

where t is time, B is the number concentration of bound particles, C is particle concentration in solution, B_0 is the bound nanoparticle concentration if the nanowire were 100 % covered, and k_a, the attachment coefficient and k_d, the detachment coefficient, kinetic constants.

Values for B were determined from the percentage coverage of the wires using the average percentage values and the geometries of the nanoparticles/ wires. The values for C were estimated based on the knowledge of the nanoparticle mass in solution, the geometry of the nanoparticles, and the density of CdSe or Au as applicable. The attachment and detachment rate coefficient was then calculated simultaneously using the information from the coverage versus time graphs of best fit. The obtained average coverage, and the lines of best fit from the obtained coefficients, are included in fig. 6.

Based on the numbers obtained the larger the CdSe nanoparticle the faster the saturation level is achieved, with the larger 24 nm x 11 nm CdSe nanoparticles having an attachment coefficient k_a of 1.67 x 10^{-18} particles^{-1} L day^{-1}, which is considerably higher than that at the 15 nm x 9 nm value of 1.60 x 10^{-19} particles^{-1} L day^{-1} and the 6 nm x 3 nm value of 1.21 x 10^{-20} particles^{-1} L day^{-1}. The detachment coefficient k_d values vary between 0.14 day^{-1}, 0.19 day^{-1}, and 0.2[illegible] day^{-1}, showing a progressive trend of easier detachment with the decrease in particle size. The continuous increases of the attachment coefficient k_a, and the decrease of the detachment coefficient k_b with nanoparticle size, for CdSe further indicate a correlation between particle size and particle attachment, suggesting that smaller nanoparticles are more susceptible to thermal excitation. Once the concentration of the nanoparticles was increased from 4.8 mg/ mL to 12.0 mg/ mL, there was an initial increase in the coverage for the 24 nm x 11 nm CdSe nanoparticles to 65 % after the first day, however; the rest of the results showed no major change with the increased concentration.

Nanoscale Accepted Manuscript

This journal is © The Royal Society of Chemistry 2015

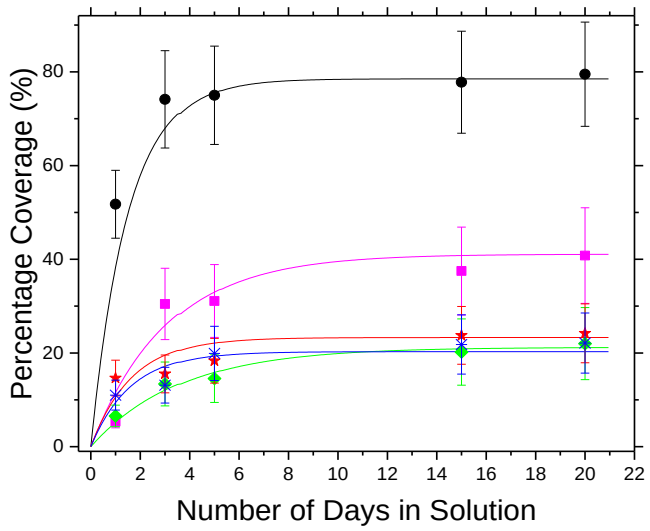

Fig. 6: The increase of the average percentage coverage for each type of nanoparticle, obtained over a period of 20 days for: (green) 6 nm x 6 nm CdSe nanoparticles, (pink) 15 nm x 9 nm CdSe nanoparticles, (black) 24 nm x 11 nm CdSe nanoparticles, (red) 19 nm diameter Au nanoparticles, and (blue) 10 nm diameter Au nanoparticles. The line of best fit for each different type of nanoparticle is displayed in its matching colour.

The reason for this can be rationalized as follows: Once the equilibrium is reached $\frac{\partial B}{\partial t} = 0$. Equation 11 becomes:

$$k_a C B_0 = B(k_a C + k_d) \qquad 12$$

This can then be divided across as:

$$B = \frac{1}{1+\frac{k_d}{k_a C}} B_0 \qquad 13$$

The initial increase in nanoparticle attachment is due to the k_aC term. Considering equation 13; however, at equilibrium it doesn't change the coverage as much, as at higher coverage the $\frac{k_d}{k_a C}$ term is much less than one, which would make the change very small.

In comparison the deposition rate coefficient of the Au nanoparticles are similar to that of CdSe nanoparticles of the closest size, with the attachment coefficient for the 19 nm nanoparticles being 7.40 x 10^{-20} particles^{-1} L day^{-1}, with a detachment coefficient of 0.46 day^{-1} and the 10 nm nanoparticles having coefficients of 3.30 x 10^{-20} particles^{-1} L day^{-1} and 0.49 day^{-1}. The difference in the results for the Au nanoparticles to that of the CdSe are attributed to increases in the interfacial lignand layer thickness, as seen in section 1, which reduce van der Waals interaction and, in turn, the number of particles which can attach to the surface. Regardless, both follow the attachment-detachment model well.

Raman Scattering

To investigate the optical properties of the completed 79.5 % covered core-shell nanowires, measurements were taken of its fluorescence and Raman peaks using a 532 nm laser at 1 mW. When the nanowire's spectrum was recorded the laser beam was positioned at the end of the wire. This allowed the Raman spectrum to be collected from the point where surface plasmon propagation would be excited, giving a good indication of the Raman enhancement afforded by the heterogeneous structure.

Investigation of the completed nanowire's optical properti indicate a fluorescence peak (supplementary information) at 620 nm with Raman bands at 210 cm^{-1}and 420 cm^{-1} corresponding to th longitudinal optical mode (LO) of the CdSe NPs and its overtone[41]. The intensities of these properties varied depending on the thickness of the silica layer demonstrating the Raman enhancement an fluorescence quenching when the metal is in close proximity to th CdSe NPs. An example of the Raman bands obtained for heterogeneous nanowire, in comparison to the CdSe monolayer is shown in Fig. 7 which gives an indication of the enhancemen t afforded by the core shell structure. The Raman bands are clearly more intense for both the 1LO and the overtone despite fewer CdSe nanoparticles being present on the nanowire's surface.

The exact level of enhancement in the Raman bands wa determined through an estimation of the Raman intensity for a individual nanoparticle. The beamwaist of the laser beam hitting th sample was calculated using the equation[42]:

$$\omega_0 = \frac{\lambda_0}{\pi NA} \qquad 14$$

Where λ_0 is the wavelength of light, NA is the numerical apert of the lens, and ω_0 is the beam waist. The beam area obtained using this equation was used to determine the number of parti illuminated in both the monolayer, and on a core-shell nanowire.

For the nanowire, this was achieved by determining the area of the wire that was covered by the laser by utilizing the averag dimension for the nanowire and the size of the beam illuminating it

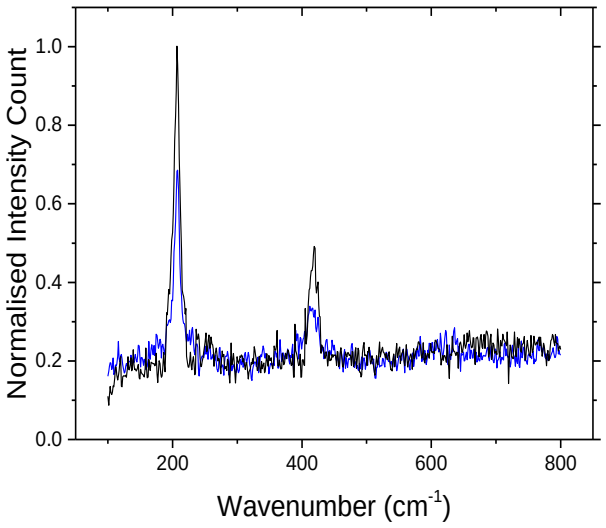

Fig. 7: Comparison of the CdSe Raman peaks for the heterogeneou nanowire (black) and the CdSe monolayer (blue). The spectra we obtained using a 532 nm laser.

In these calculations the tip of the nanowire was taken to be ne the edge of the beam's circumference. Using the dimensions of the nanoparticle, the number of particles capable of covering 79.5 % the nanowire's surface in this region was calculated.

The number of nanoparticles was then used to determine th individual Raman band contribution from a single CdSe nanoparticl This contribution was calculated for both of the CdSe bands in th spectra from multiple nanowires. These values were then compare with the individual contributions from three different Cas

Nanoscale Accepted Manuscript

monolayer reference readings, and used to determine the percentage increase in each case. For both the LO and its overtone the intensity factor for the core-shell nanowire nanoparticles was found to be much higher than the nanoparticle monolayer. Values for the LO band showed an average increase of 141.27 % (or a ratio of 2.41) in individual CdSe intensity for the nanowires, with typical values between 90 and 190 %. The overtone itself showed an average intensity increase of 85.86 % (ratio of 1.85) per nanoparticle, with the majority of wires having increases between 60 and 90 %. These observed increases are due to the electric field enhancement after the excitation of surface plasmon propagation, increasing the signal strength per nanoparticle (see supplementary information).

In order to determine the exact effect on the electron phonon interactions for these wires the Huang-Rhys factor S was calculated, which gives a measurement of the Fröhlich interaction. The S-factor is equivalent to $\Delta^2 = \sum_k \Delta_k^2$ where Δ_k is the shift of the harmonic oscillator potential when coupling between phonons is treated as Hamiltonian[42].

The ratio of integrated intensities for the first and second LO overtones can be used to obtain Δ for a given system. In these calculations the excitation effective mass was taken as $M^* = (1/ m_e + 1/ m_h)^{-1} = 0.112$[41]. The S-factor of the nanowires was found to have values between 0.043 and 0.054, in comparison to the S-factor of the CdSe monolayer which had a typical value of 0.039. The change in S-factor is due to alterations in the confining potential for the electron hole wave function[44,45]. Similar to the intensity increase, the main factor for the change in S value is the silica layer thickness. Variations in the insulator affect the way that the metallic and semiconductor layers interact, resulting in various S-factors.

Conclusions

CdSe-silica-silver nanowires were successfully synthesized using a new heteroaggregation assisted wet synthesis route. Results obtained from the heteroaggregation indicate that the larger 24 nm x 11 nm CdSe nanoparticles are capable of covering an average of 79.5 % of the surface corresponding to a completed structure. The increase of coverage due to particle size is attributed to increases in the van der Waals attractive force, resulting in a much deeper energy well and making it harder for the nanoparticles to escape back into solution. However, increased ligand length can greatly diminish this effect and lead to lower particle coverage on the nanowire surface, as demonstrated in the Au-silica-silver nanowire cases. Our study provides general guidance on the factors that need to be considered in particle-nanowire attachment in a nonpolar environment. The attachment rate, and saturation point are dependent on the attachment and detachment rate of nanoparticles reaching equilibrium, in turn related to the depth of the energy well.

Analysis of the completed wires highlight an increase in the intensity of the Raman peaks of CdSe for the completed heterogeneous nanowires in comparison to the plain nanoparticles, due to the generated surface plasmon propagation. The unique shape and Raman enhancement offered by these nanowires makes their advantageous attributes over plain metal nanowires for incorporation into sensor tips. It is expected that they could perform well as probe tips in microscopy techniques[46] such as near field optical microscopy, and in chemical analysis, due to their strong Raman bands. In addition, the possibility also exists to use the nanowires to functionalize certain biological microorganisms; allowing their processes in drug delivery to be studied in detail.

Acknowledgements

I. Pita would like to acknowledge funding from the Irish Research Council: GOIPG/58/2013. Thanks to Louise Barry for assistance with nanoparticle synthesis. S. Singh thanks the support from Irish Government's Programme for Research in Third Level Institutions Cycle 5, National Development Plan 2007–2013 with the assistance of the European Regional Development Fund

Notes and references

1 R. Neil, W. Macpherson and J. V., *Nat. Nanotechnol.*, 2009, **4**, 483-491
2 H. Wei, Z. Wang, X. Tang, M. Käll, and H. X. Xu, *Nat. Commum.*, 2011, **2**, 2:387
3 Y. R. Fang and M. T. Sun, *Light: Sci. Appl.* 2015, **4**, e294
4 Y. Z. Huang, Y. R. Fang, Z. L. Zhang, L. Zhu and M. T. Sun, *Light: Sci. Appl*. 2014, **3**, e199
5 M. Singh, D. Movia, O. K. Mahfoud, Y. Volkov, and A. Prina-Mello, *Eur. J. Nanomed.*, 2013, **5(4)**, 195-204
6 W. Barnes, A. Dereux, and T. W. Ebbesen, *Nature*, 2003, **424**, 824-830
7 N. Liu, H. Wei, J. Li, X. Tian, A. Pan, and H. Xu, *Sci. Rep.*, 2013, **3**, 3:1967
8 R. F. Oulton, V. J. Sorger, T. Zentgraf, R. Ma, C. Gladden, L. Dai, G. Bartal, and X. Zhang, *Nature*, 2009, **461**, 629-632
9 J. Yang, H. I. Elim, Q. Zhang, J. Y. Lee, and W. Li, *J. Am. Chem. Soc.*, 2006, **128**, 11921-11926
10 C. Shen, L. Wu, S. Zhang, H. Ye, B. Li, and Y. Huang, *J. Colloid Interface Sci.*, 2014, **421**, 103-113
11 P. Dušak, A. Mertelj, S. Kralj, and D. J. Makovec, *J. Colloid Interface Sci.*, 2015, **438**, 235-243
12 I. L. Radtchenko, B. S. G., N. Gaponik, A. Kornowski, A. L. Rogach, and H. Möhwald, *Adv. Mater.*, 2001, **13,** 1684-1687
13 J. H. Lee, A. M. M., V. Sitterle, J. Sitterle, and J. C. J. Meredith, *J. Am. Chem. Soc.*, 2009, **131**, 5048-5049
14 P. Linse, and H. Wennerström, *Soft Matter*, 2012, **8**, 2486-2493
15 S. M. Kang, K. B. Lee, D. J. Kim, and I. S. Choi, *Nanotechnology*, 2006, **17**, 4719
16 S. H. Liu, and M. Y. Han, *Adv. Func. Mater.*, 2005, **15**, 961
17 W. Stöber, A. Fink, and E. J. Bohn, *J. Colloid and Interface Sci.*, 1968, **26**, 62-69
18 Y. Yin, Y. Lu, Y. Sun, and Y. Xia, *Nano Lett.*, 2002, **2**, 427-430
19 S. Ahmed and K. M. Ryan, *Adv. Mater.* 2008, **20**, 4745-4750
20 A. Singh, N. J. English and K. M. Ryan, *J. Phys. Chem. B*, 2013, **117**, 1608-1615
21 Z. Chen, J. Moore, G. Radtke, H. Sirringhaus, and S. O'Brien, *J. Am. Chem. Soc*., 2007, **129**, 15702
22 Y. Sun, and Y. Xia, *Adv. Mater.*, 2002, **14**, 833-837
23 A. Singh, R. D. Cunning, S. Ahmed, C. A. Barrett, N. J. English, J. A. Garate, and K. M. Ryan, *J. Mater. Chem.*, 2012, **22**, 1562-1569
24 I. Gur, N. A. Fromer, M. L. Geier, and A. P. Alivisatos, *Science*, 2005, **310**, 462-465
25 H. Hiramatsu, and F. E. Osterloch, *Chem. Mater.*, 2004, **16**, 2509-2511
26 J. N. Israelachivili, *Intermolecular and Surface Forces 3rd Ed* Academic Press Elsevier, Netherlands, 2011
27 G. Lefèvre, and A. Jolivet, *Calculation of Hamaker Constants Applied to the Deposition of Metallic Oxide Particles at High Temperature*, Proceedings of the International Conference on Heat Exchanger Fouling and Cleaning VIII, Austria, 2009
28 S. Eichenlaub, C. Chan, and S. P. Beaudoin, *J. Colloid Interface Sci.*, 2002, **248**, 389-397

Nanoscale Accepted Manuscript

 This journal is © The Royal Society of Chemistry 2015

29 C. S. Chen, *Principles and Applications of Emulsion Polymerisation*, Wiley, New Jersey, 2008
30 J. H. Masliyah, and S. Bhattacharjee, *Electrokinetic and Colloid Transport Phenomena*, Wiley, New Jersey, 2006
31 G. Ge, and L. Brus, *J. Phys. Chem. B*, 2000, **104**, 9573-9575
32 P. C. Heimenz, and R. Rajagopalan, *Principles of Colloid and Surface Chemistry 3rd Ed.*, Marcel Dekker, New York, 1997
33 M. Ruths, and J. N. Israelachivili, in *Nanotribology and Nanomechanics*, ed. B. Bhushan, Springer, Germany, 2011, Chapter 13, p. 112
34 K. Li, and Y. Chen, *Colloids and Surfaces A. Physiochem. Eng. Aspects*, 2012, **415**, 218-229
35 Y. Gu, and D. Li, *J. Colloid Interface Sci.*, 1999, **217**, 60-69
36 S. Bhattacharjee, and M. J. Elimelech, *J. Colloid Interface Sci.*, 1997, **193**, 273-285
37 D. J. McClements, *Nanoparticle- and Microparticle- based Delivery Systems: Encapsulation, Protection, and Release of Active Compounds*, CRC Press, Florida, 2014
38 J. Rosen, *Encyclopaedia of Physics*, Infobase Publishing, New York, 2009
39 J. K. T. Quik, I. Velzeboer, M. Wouterse, A. A. Koelmans, and D. van der Meent, *Water Res.*, 2014, **48**, 269-279
40 M. J. Kim, and K. Rhee, *Effects of Spatial Shear Gradient on Nanoparticle Adhesion to the Endothelium*, IFMBE Proceedings, New York, 2012
41 R. Venugopal, P. Lin, C. C. Liu, and Y. T. Chen, *J. Am. Chem. Soc.*, 2005, **127**, 11262-11268
42 J. C. Daly, *Fiber Optics*, Science Publishing, Banbury U. K., 1984
43 G. Scamarcio, V. Spagnolo, G. Ventruti, and M. Lugará, *Phys. Rev. B.*, 1996, **53**, R10489-R10491
44 K. D. Krauss, and F. W. Wise, *Phys. Rev. B*, 1997, **55**, 9860-9865
45 H. Lange, M. Artemyev, U. Woggon, T. Niremann, and C. Thomsen, *Phys. Rev. B.*, 2008, **77**, 193303-1-193303-4
46 Y. Nakayama, P. J. Pauzauskie, A. Radenovic, R. M. Onorato, R. J. Sakally, J. Liphardt, and P. Yang, *Nature*, 2007, **447**, 1098-1101

Nanoscale Accepted Manuscript